N87-20279

THE CHEMICAL SHOCK TUBE AS A TOOL FOR STUDYING HIGH-TEMPERATURE CHEMICAL KINETICS

Theodore A. Brabbs
NASA Lewis Research Center
Cleveland, Ohio

Although the combustion of hydrocarbons is our primary source of energy today, the chemical reactions, or pathway, by which even the simplest hydrocarbon reacts with atmospheric oxygen to form CO_2 and water may not always be known. Furthermore, even when the reaction pathway is known, the reaction rates are always under discussion. The shock tube has been an important and unique tool for building a data base of reaction rates important in the combustion of hydrocarbon fuels.

The ability of a shock wave to bring the gas sample to reaction conditions rapidly and homogeneously makes shock-tube studies of reaction kinetics extremely attractive. In addition to the control and uniformity of reaction conditions achieved with shock-wave methods, shock compression can produce gas temperatures far in excess of those in conventional reactors. Argon can be heated to well over 10 000 K, and temperatures around 5000 K are easily obtained with conventional shock-tube techniques. Experiments have proven the validity of shock-wave theory; thus, reaction temperatures and pressures can be calculated from a measurement of the incident shock velocity.

This report presents a description of the chemical shock tube and auxiliary equipment and of two examples of kinetic experiments conducted in a shock tube. Shock-wave theory and shock tubes in general are discussed in references 1 and 2 and thus are not included in this report.

EXPERIMENTAL APPARATUS AND PROCEDURES

The chemical shock tube used was a single piece of square stainless-steel tubing (5.7 m long, 6.4 cm on a side, 1.3 cm thick walls). The entire length of the tube was ground to a constant inside dimension and then honed to a highly polished finish. Stations for shock-wave detectors were located at 15-cm intervals in the downstream portion of the tube. Two 2.5-cm calcium fluoride windows were located 25 cm from the end of the tube. A quartz pressure transducer was located at a position where it would provide an accurate indication of the time at which a shock wave arrived at the center of the windows. The assembled tube could be evacuated to a pressure of about 1 μm and had a leak rate of less than 0.2 μm/min. A liquid nitrogen cold trap in the vacuum line guarded against the back-migration of pump oil into the shock tube.

The temperature and pressure behind the incident and reflected shock waves were calculated from the measured velocity of the incident shock wave with the shock program of Gordon and McBride (ref. 3). Since the reaction temperature had to be calculated, it was very important to measure the initial temperature and the shock velocity as accurately as possible. The distances between probe locations were accurately measured to four significant figures. The shock-tube wall temperature was measured to ±0.5 C, and it was assumed that the test mixture rapidly achieved this temperature. Thin-film resistance gauges (1.3 cm

diam) were used to detect the passage of the incident shock wave. The amplified output from these gauges was displayed on a digital oscilloscope (see fig. 1). Data points were recorded every 200 nsec. Since with this scope the scale can be magnified to allow viewing of each point, we were able to measure the incident shock velocity to better than ±0.2 μsec (0.1 percent).

All data were taken at an initial test gas pressure of 8.00 kPa (60 torr) and a driver pressure of 792.7 kPa (115 psia). Soft aluminum diaphragms separated the high-pressure driver gas from the test gas. These diaphragms were pressurized and then pierced by a gas-activated piston. The shock strength was varied by adding small amounts of argon to the helium driver gas to change its molecular weight. Figure 2 shows the variation of shock velocity with the reciprocal of the molecular weight of the driver gas. The constant pressure ratio across the diaphragm insured that the opening process for the diaphragm was about the same for all tests.

Gas mixtures were prepared by the method of partial pressures in 34.4-liter stainless-steel tanks. The gases used to prepare the mixtures had stated purities of 99.99-percent methane, 99.98-percent oxygen, and 99.998-percent argon. The partial pressure of methane and oxygen could be determined to better than 0.3 mm of Hg, and the total pressure of the tank to better than 1.38 kPa (0.2 psia). All samples were prepared to a total pressure of 413.6 kPa (60 psia).

Radiation at 3700 Å was monitored for each experiment and was displayed on the oscilloscope with the pressure history. The radiation was detected by a photomultiplier tube whose field of view was restricted by two slits (0.75 and 1.5 mm wide) located 10 and 23 cm from the center of the shock tube. With this arrangement we could view a 3-mm slice of the hot gas in the center of the shock tube at the same location as the pressure transducer. An interference filter centered at 3696.5 Å (with a half band width of 115 Å) was used to isolate the 3700 Å radiation. The filter transmitted 51 percent of the incident radiation.

Examples of kinetic experiments conducted in a shock tube are presented in the next two sections.

SHOCK TUBE MEASUREMENTS OF SPECIFIC REACTION RATES IN THE BRANCHED-CHAIN H_2-CO-O_2 SYSTEM

When a mixture containing hydrogen, carbon monoxide, and oxygen is subjected to a temperature and pressure pulse in a shock tube, small concentrations of atoms and free radicals are first formed by processes such as

$$CO + O_2 \longrightarrow CO_2 + O$$

These concentrations may then grow exponentially via the well-known branched-chain scheme

$$OH + H_2 \xrightarrow{k_1} H_2O + H \qquad \text{I}$$

$$H + O_2 \xrightarrow{k_2} OH + O \qquad \text{II}$$

$$O + H_2 \xrightarrow{k_3} OH + H \qquad \text{III}$$

$$H + O_2 + M \xrightarrow{k_4} HO_2 + M \qquad \text{IV}$$

$$OH + CO \xrightarrow{k_5} CO_2 + H \qquad \text{V}$$

Theory shows (refs. 4 and 5) that the oxygen atom concentration grows as $[O] \cong A \exp \lambda t$, (except very early in the reaction). Where λ is the positive root of the cubic equation

$$\lambda^3 + (\nu_1 + \nu_2 + \nu_3 + \nu_4 + \nu_5)\lambda^2 + [(\nu_1 + \nu_5)(\nu_3 + \nu_4) + \nu_3\nu_4]\lambda - \nu_3(\nu_1 + \nu_5)(2\nu_2 - \nu_4) = 0 \qquad (1)$$

where $\nu_1 \equiv k_1[H_2]$, $\nu_2 \equiv k_2[O_2]$, $\nu_3 \equiv k_3[H_2]$, $\nu_4 \equiv k_4[O_2][M]$, and $\nu_5 \equiv k_5[CO]$.

Thus, the exponential growth constant λ depends on the gas composition and the rate constants of reactions I to V. This paper reports measurements of mixtures chosen to permit determination of the rates of reactions I, II, III, and V. Mixtures were selected by analyzing equation (1).

Growth constants were obtained by measuring the blue carbon monoxide flame-band emission behind incident shocks. The intensity of this radiation is proportional to the product of carbon monoxide and oxygen atom concentrations (ref. 6), and, since very little carbon monoxide is consumed, the light monitors the increase of oxygen atom concentration with time. A typical emission record is presented in figure 3.

Exponential growth constants were obtained from plots of the logarithm of observed light intensity as a function of gas time (see fig. 4); the relation between gas and laboratory times was obtained from the computer calculations.

SELECTION OF GAS MIXTURES

Let us turn now to the rationale used to select gas mixtures by analyzing equation (1). To begin with, under our experimental conditions ν_4 is generally small in comparison with other ν; therefore, it can be neglected for purposes of a qualitative discussion. Secondly, λ turns out to be a small positive root - of the order of the smaller ν values and very small compared with the larger ν values. Thus, we neglect λ^3 in comparison with the other terms and rewrite equation (1) as

$$[(\nu_1 + \nu_5) + \nu_2 + \nu_3]\lambda^2 + \nu_3(\nu_1 + \nu_5)\lambda \cong 2\nu_2\nu_3(\nu_1 + \nu_5) \qquad (2)$$

If the amount of hydrogen in a mixture is large in comparison to the amount of oxygen, v_1 and v_3 are large and the term involving λ^2 may be neglected; in this event,

$$\lambda \simeq 2v_2 \tag{3}$$

On the other hand, if only a trace of hydrogen is present; v_3 is small, the term involving λ may be neglected, and

$$\lambda^2 \simeq \frac{2v_2v_3(v_1 + v_5)}{v_2 + (v_1 + v_5)} \tag{4}$$

If we choose a mixture with a large amount of carbon monoxide, v_5 is large and

$$\lambda \sim \sqrt{2v_2v_3} \tag{5}$$

If there is a large amount of oxygen, v_2 is large and

$$\begin{aligned} &\lambda \sim \sqrt{2v_3(v_1 + v_5)} \\ &\lambda \sim \sqrt{2v_3v_1} \qquad \text{for} \qquad [H_2] > [CO] \\ &\lambda \sim \sqrt{2v_3v_5} \qquad \text{for} \qquad [CO] > [H_2] \end{aligned} \tag{6}$$

This, then, outlines a strategy for obtaining rates of reactions I, II, III, and IV. First, a mixture rich in hydrogen is used to determine k_2. Next, with k_2 known, a mixture with a trace of hydrogen and rich in carbon monoxide is used to determine k_3. Finally, with k_3 known, mixtures with excess oxygen and varying proportions of hydrogen and carbon monoxide are used to isolate k_1 and k_5.

The foregoing discussion indicates a qualitative procedure for selecting gas mixtures. However, we also need a quantitative measure of the sensitivity of the growth constant for a particular mixture to the various rate constants. For example, we know that to isolate k_3 we need a mixture with a trace of hydrogen, a small amount of oxygen, and an excess of carbon monoxide. But, for a candidate composition, is the hydrogen concentration small enough, and is carbon monoxide sufficiently in excess? A quantitative measure of the sensitivity to the various rates can be obtained by logarithmic partial differentiation of equation (1). For example,

$$\left(\frac{\partial \ln \lambda}{\partial \ln v_3}\right) = \frac{1}{2} - \frac{1}{2}\left[\frac{\lambda^2 + 2v_3\lambda + (v_1 + v_5)(v_3 - v_4) + v_3v_4}{3\lambda^2 + 2(v_1 + v_2 + v_3 + v_4 + v_5) + (v_1 + v_5)(v_3 + v_4) + v_3v_4}\right] \tag{7}$$

Equation (7) shows that the growth constant depends on something less than $\sqrt{v_3}$ (a somewhat weaker dependence than that suggested by equation (5)).

The mixture compositions selected are shown in table I along with the sensitivities calculated for a pressure of 1 atmosphere and the temperatures near the midpoints of the ranges of the experimental data. These mixtures were chosen on the basis of (1) high sensitivity to the rate constant being determined, (2) minimized sensitivity to the other rate constants, (3) growth constants in a convenient range for measurement (5×10^3 to $7 \times 10^4 sec^{-1}$), and (4) sufficient content of minor, rate-limiting constituents to permit accurate mixture preparation.

It was necessary to include in each mixture sufficient infrared-active gas so that the arrival of the contact surface could be detected by the cessation of infrared emission. (The position of the contact surface between the driver and the driven gas was needed for the boundary layer analysis.) Mixtures 2, 3, and 5 have substantial carbon monoxide concentrations; carbon dioxide was added to mixture 1 to achieve adequate infrared activity. Carbon dioxide was also added to mixtures 3 and 5 to ensure vibrational relaxation of the carbon monoxide. In preliminary experiments on a composition similar to mixture 3 (both without CO_2) carbon monoxide was not relaxed and rate constants gave an activation energy of 15 kcal for reaction 3; this is much higher than the values shown in reference 7. Results from mixture 3, with added CO_2, show that the preliminary data were too low (particularly at the lower temperatures).

CALCULATION OF RATE CONSTANTS FROM EXPONENTIAL GROWTH CONSTANTS

Rate constants were obtained from the experimental growth constants by means of equation (1), which was rearranged and solved for the rate constant being sought from the mixture in question: k_2 from mixture 2, k_3 from mixture 3, etc. Mixture 2 was studied first, because the growth constants for this mixture depend almost exclusively on k_2 and are only slightly affected by the rates of the other reactions (table 1). Values of ν_4 were calculated from the k_4 suggested by the Leeds Group (ref. 8). Trial values of k_1, k_3, and k_5 were also taken from the Leeds recommendations (refs. 7 to 9), but final values were taken from our own determinations. This involves an iterative procedure since our values of k_3 depend, in turn, on our values of k_2 and, to a lesser extent, of k_5. Two iterations sufficed to establish k_2.

Next, k_3 was obtained by analyzing the growth constants for mixture 3, then k_1 was obtained from mixture 1, and finally k_5 was obtained from mixture 5. Three iterations around the k_3-k_1-k_5 loop were required.

A least-squares fit to the Arrhenius equation was made for each set of rate constants; these equations were then used in subsequent calculations.

The experimental results are presented in the order in which the data were obtained - first k_2, then k_3, k_1, and k_5. This is also the order of decreasing precision.

Rate constants for reactions II and III are plotted as functions of reciprocal temperature in figure 5. The least-squares lines through the data are

$$k_2 = 1.25 \times 10^{14} \exp(-16.3 \text{ kcal/RT}) \text{ cm}^3 \text{ mole}^{-1} \text{ sec}^{-1}$$
$$k_3 = 2.96 \times 10^{13} \exp(-9.8 \text{ kcal/RT}) \text{ cm}^3 \text{ mole}^{-1} \text{ sec}^{-1}$$

Figure 6 contains the data for reactions I and V plotted as functions of the reciprocal temperature. The least-squares lines through the data are

$$k_1 = 1.9 \times 10^{13} \exp(-4.8 \text{ kcal/RT}) \text{ cm}^3 \text{ mole}^{-1} \text{ sec}^{-1}$$
$$k_5 = 1.0 \times 10^{12} \exp(-3.7 \text{ kcal/RT}) \text{ cm}^3 \text{ mole}^{-1} \text{ sec}^{-1}$$

In this paper we showed how to make systemmatic measurements so as to isolate the rates of individual bimolecular reaction steps in the complex of six reactions which describe the ignition behavior of the hydrogen-carbon monoxide-oxygen system.

We have obtained what we believe are quite accurate measurements of the rates of the reactions $H + O_2 \rightarrow OH + O$ and $O + H_2 \rightarrow OH + H$. Proper accounting of the effects of boundary layer growth on the pressure, temperature, and residence time behind the shock wave has been essential. Our measurements of the rates of $OH + H_2 \rightarrow H_2O + H$ and $OH + CO \rightarrow CO_2 + H$ were less precise but were perhaps the most direct determinations of these rates for temperatures above 1100 K (previous high-temperature determinations of these rates have been based on flame sampling). Finally, we have estimated the rate of the initiation reaction $CO + O_2 \rightarrow CO_2 + O$.

METHANE OXIDATION BEHIND REFLECTED SHOCK WAVES, IGNITION DELAY TIMES MEASURED BY PRESSURE AND FLAME-BAND EMISSION

Large computers have enabled us to assemble kinetic mechanisms for modeling the combustion of many fuels. These mechanisms may have as many as 150 reactions (variables) and in some cases the only experimental parameter matched has been the ignition delay times obtained from shock tubes. Many studies have been conducted on the ignition of methane-oxygen gas mixtures in shock tubes. However, in some cases the data are in error because of probe location, and in other cases the data are badly scattered because of poor measurements of the incident shock velocity or a very noisy pressure trace.

The delay time measured for a shock-heated hydrocarbon-oxygen mixture is known to be a function of initiation reactions, of reactions of radicals and molecular oxygen with the fuel, and of branching reactions. These branching reactions increase the radical concentrations to a level where ignition will occur. During ignition, there is rapid depletion of the primary fuel, very high radical concentrations, and an exponential rise in temperature and pressure. Usually delay times are measured somewhere in this region by techniques which follow some physical process such as change in pressure or in the appearance of some emitting species. Although the time difference between the start and completion of the pressure rise is small, one would like to determine the time of the appearance of the signal as accurately as possible. This time, which is the start of the ignition process, allows one to separate the fast ignition mechanism from the kinetics of the primary fuel.

The next section presents ignition delay data for the oxidation of methane. Data were measured with a quiet pressure transducer for the temperature range of 1500 to 1920 K. The quiet pressure trace allowed us to determine the initial rise in the ignition pressure. The delay times determined from this initial pressure rise were compared with the time of appearance of the

radiation at 3700 Å. In addition, the methane and carbon dioxide concentrations at the time of ignition will be measured. These parameters, which must be duplicated by any kinetic model, will be used to test the correctness of published kinetic models for the combustion of methane.

RESULTS AND DISCUSSION

Ignition Delay Times and Probe Location

Frenklach (ref. 10) measured ignition delay times at two locations in a shock tube and concluded that the location of the probe must be taken into consideration when selecting delay-time data to be modeled by a kinetic mechanism. Since optical access was necessary to monitor the infrared and ultraviolet radiation behind the reflected shock wave, it was important to know the error involved in measuring the delay time 7 mm from the reflecting surface. Therefore, two pressure transducers were located 7 and 83 mm from the reflecting surface. These allowed us to simultaneously measure the delay time for two locations in the same experiment (see fig. 7). An ethane-oxygen-argon mixture (1.27, 5.05, and 93.68 percent, respectively) was used for this series of tests. For these experiments, delay time was defined as the time at which the ignition pressure exceeded P_5 by 10 percent. This eliminated the guess-work usually involved in determining the point at which the pressure departed from the flat portion of the trace. Figure 8 is a plot of the delay times for the two locations as a function of 1/T. A curve drawn through the data taken at the 83-mm position appears to show a constant difference in the time between the two locations.

A clearer understanding of this phenomenon can be obtained from figure 9, which is a time-distance (t-x) plot of the trajectory of the incident and reflected shock waves near the end of the shock tube. As can be seen, the time at which shock heating occurs at a given location along the tube is a function of the reflected shock velocity and the distance from the end wall. Thus, ignition would be expected to occur at the end wall first, since the gas there has been heated much longer. When ignition occurs, the pressure rise causes a disturbance which propagates down the tube. The mininum propagation velocity of this disturbance is the speed of sound in the shocked gas. Vermeer (ref. 11) took schlieren photographs of ignition behind the reflected shock wave, and they clearly showed that the disturbance propagated at a velocity much greater than the reflected shock wave.

The data in figure 8 were used to calculate the propagation velocity between the two probes. This velocity had an average value of 1660 m/sec, which is a Mach number of about 2.5. This velocity is about four times that of the reflected shock wave. Using this velocity one can estimate that the delay times measured at the 7-mm position would be too short by about 10 μsec. This error would not be important unless the measured delay times were near 100 μsec. No corrections have been made in the present data, but times less than 100 μsec are not considered reliable.

Another disturbing feature of the pressure traces is the amplitude of the ignition pressure. Unless something changes, one expects the ignition pressure to be the same at all locations in the tube. However, the ignition pressure for probe 2 is much larger than that at probe 1 (fig. 4). The ratio of the

ignition pressure to the reflected shock pressure P_5 for the two probe positions is plotted as a function of the delay time at probe 1 in figure 10. Note that this ratio is nearly constant at probe 1 but increases with decreasing delay times for probe 2. This behavior suggests that the gas properties at ignition are not the same at the two locations.

Ignition Delay Times

Ignition delay times were measured behind reflected shock waves for the mixtures shown in table II. The pressure history and the carbon monoxide flame-band emission at 3700 Å were used to determine the onset of ignition. The delay times measured by both pressure and flame-band emission are recorded in table III. These delay times τ may be correlated by an empirical relation of the form

$$\tau = A \exp(B/RT)[CH_4]^a[O_2]^b[Ar]^c \tag{8}$$

Lifshitz (ref. 12) and Tsuboi (ref. 13) both found an overall pressure dependence of -0.7 for $a + b + c$. Plots of $\tau P^{0.7}$ as a function of $1/T$ for each mixture are shown in figure 8. A least-squares fit to the data yielded the following equations:

$$\varphi = 0.5 \quad \tau P^{0.7} = 9.59\times10^{-5} \exp(51.93\times10^3/RT) \ \mu\text{sec-atm}^{0.7} \tag{9}$$

$$\varphi = 1.0 \quad \tau P^{0.7} = 2.85\times10^{-5} \exp(58.83\times10^3/RT) \ \mu\text{sec-atm}^{0.7} \tag{10}$$

$$\varphi = 2.0 \quad \tau P^{0.7} = 3.65\times10^{-5} \exp(58.74\times10^3/RT) \ \mu\text{sec-atm}^{0.7} \tag{11}$$

A correlation of all of the data in the form used by Lifshitz, $\tau[CH_4]^{-0.33}[O_2]^{1.03}$, is shown in figure 11. The activation energies for the present data were larger than those found by Lifshitz and appear to have depended upon the concentration of oxygen. The mixtures of $\varphi = 1.0$ and 2.0 had 4-percent oxygen and the same activation energy, while the mixture for $\varphi = 0.5$ had 8-percent oxygen and a measurably lower activation energy. This is the same behavior reported by Tsuboi.

REFERENCES

1. Gaydon, A.G; and Hurle, I.R.: The Shock Tube in High-Temperature Chemical Physics. Reinhold Publishing, 1963.

2. Greene, E.F.; and Toennies, J.P.: Chemical Reactions in Shock Waves. Academic Press, 1964.

3. Gordon, S; and McBride, B.J.: Computer Program for Calculation of Complex Chemical Equilibrium Compositions, Rocket Performance, Incident and Reflected Shocks, and Chapman-Jouguet Detonations. NASA SP-273, 1976.

4. Brokaw, R.S.: Analytic Solutions to the Ignition Kinetics of the Hydrogen-Oxygen Reaction. Tenth Symposium (International) on Combustion, The Combustion Institute, 1965, pp. 269-278.

5. Brokaw, R.S.: Ignition Kinetics of the Carbon Monoxide-Oxygen Reaction. Eleventh Symposium (International) on Combustion, The Combustion Institute, 1967, pp. 1063-1073.

6. Clyne, M.A.A.; and Thrush, B.A.: Mechanism of Chemiluminescent Combination Reactions Involving Oxygen Atoms. Proc. Roy. Soc. (London), Ser. A, vol. 269, no. 1338, Sept. 25, 1962, pp. 404-418.

7. Baulch, D.L.; Drysdale, D.D.; and Lloyd, A.C.: Critical Evaluation of Rate Data for Homogeneous, Gas-Phase Reactions of Interest in High Temperature Systems. High Temperature Reaction Rate Data, vol. 2, Dept of Physical Chemistry, The University Leeds, Nov. 1968.

8. Baulch, D.L.; Drysdale, D.D.; and Lloyd, A.C.: Critical Evaluation of Rate Data for Homogeneous, Gas-Phase Reactions of Interest in High Temperature Systems. High Temperature Reaction Rate Data, vol. 3, Dept of Physical Chemistry, The University, Leeds, Apr. 1969.

9. Baulch, D.L.; Drysdale, D.D.; and Lloyd, A.C.: Critical Evaluation of Rate Data for Homogeneous, Gas-Phase Reactions of Interest in High Temperature Systems. High Temperature Reaction Rate Data, vol. 1, Dept. of Physical Chemistry, The University, Leeds, May 1968.

10. Frenklach, M.; and Bornside, D.E.: Shock-Initiated Ignition in Methane-Propane Mixtures. Combust. Flame, vol. 56, no. 1, Apr. 1984, pp. 1-27.

11. Vermeer, D.J.; Meyer, J.W.; and Oppenheim, A.K.: Auto-Ignition of Hydrocarbons Behind Reflected Shock Waves. Combust. Flame, vol. 18, no. 3, June 1972, pp. 327-336.

12. Lifshitz, A., et al.: Shock-Tube Investigation of Ignition in Methane-Oxygen-Argon Mixtures. Combust. Flame, vol. 16, no. 3, June 1971, pp. 311-321.

13. Tsuboi, T.; and Wagner, H.G.: Homogeneous Thermal Oxidation of Methane in Reflected Shock Waves. Fifteenth Symposium (International) on Combustion, The Combustion Institute, 1971, pp. 883-890.

TABLE I. - MIXTURE COMPOSITIONS AND GROWTH CONSTANT SENSITIVITIES

Constituents	Mixture			
	1	2	3	5
	Reaction			
	$OH + H_2 \rightarrow H_2O + H$	$H + O_2 \rightarrow OH + O$	$O + H_2 \rightarrow OH + H$	$OH + CO \rightarrow CO_2 + H$
	Composition, percent			
H_2	0.21	5	0.1046	0.1035
CO	.11	6	10.0	6.01
O_2	10.0	0.5	.503	10.0
CO_2	5.0	- -	4.99	5.0
Sensitivities	Mixture			
	1	2	3	5
	Reaction			
	$OH + H_2 \rightarrow H_2O + H$	$H + O_2 \rightarrow OH + O$	$O + H_2 \rightarrow OH + H$	$OH + CO \rightarrow CO_2 + H$
$(\partial \ln \lambda)/(\partial \ln \nu_1)$	0.34	0.01	0.00	0.07
$(\partial \ln \lambda)/(\partial \ln \nu_2)$	.33	1.00	.64	.21
$(\partial \ln \lambda)/(\partial \ln \nu_3)$	.48	.06	.39	.49
$(\partial \ln \lambda)/(\partial \ln \nu_4)$	-.17	-.07	-.06	-.06
$(\partial \ln \lambda)/(\partial \ln \nu_5)$	.02	.00	.04	.29

TABLE II. - COMPOSITION OF GAS MIXTURES AND TEMPERATURE RISE DUE TO IGNITION

Equivalence ratio, φ	CH_4	O_2	Ar	Temperature rise due to ignition, K
	Composition, percent			
0.50	2	8	90	894
1	2	4	94	882
2	4	4	92	729

TABLE III. - IGNITION DELAY TIMES MEASURED BY PRESSURE AND FLAME BAND EMISSION

(a) Equivalence ratio, φ, 0.5; methane, 2 percent; oxygen, 8 percent; argon, 90 percent

Temperature, K	$1/T$, K^{-1}	Pressure, atm	Delay times, μsec	
			Pressure	Emission
1778	5.624×10^{-4}	3.464	99	110
1763	5.672	3.418	102	110
1752	5.708	3.371	112	125
1730	5.780	3.318	159	167
1695	5.900	3.199	201	208
1687	5.928	3.191	208	209
1657	6.035	3.072	323	322
1620	6.173	2.979	508	512
1610	6.211	2.950	533	542
1605	6.231	2.918	594	597
1601	6.246	2.922	672	672
1579	6.333	2.857	663	658
1576	6.345	2.835	742	738
1555	6.431	2.773	850	858
1554	6.435	2.786	958	964
1531	6.532	2.704	1144	1145
1499	6.671	2.613	1655	1649

TABLE III. - Concluded.

(b) Equivalence ratio, φ, 1.0; methane, 2 percent; oxygen, 4 percent; argon, 90 percent

Temperature, K	1/T, K^{-1}	Pressure, atm	Delay times, μsec	
			Pressure	Emission
1915	5.222×10^{-4}	3.680	57	59
1866	5.359	3.536	84	78
1802	5.549	3.354	171	166
1780	5.618	3.279	201	219
1775	5.638	3.278	185	192
1746	5.727	3.183	295	295
1732	5.774	3.147	383	383
1725	5.797	3.122	397	396
1710	5.848	3.082	427	414
1707	5.858	3.077	531	559
1689	5.921	3.023	525	522
1689	5.921	3.032	589	589
1655	6.042	2.932	794	775
1645	6.079	2.900	867	861
1635	6.116	2.876	967	973
1629	6.139	2.855	1072	1075
1615	6.192	2.822	1163	1144
1593	6.278	2.761	1448	1471

(c) Mixture ratio, φ, 2.0; methane, 4 percent; oxygen, 4 percent; argon, 92 percent

Temperature, K	1/T, K^{-1}	Pressure, atm	Delay times, μsec	
			Pressure	Emission
1922	5.203×10^{-4}	4.012	67	62
1856	5.388	3.797	116	110
1789	5.590	3.583	198	201
1770	5.650	3.524	249	271
1763	5.672	3.485	318	304
1730	5.780	3.381	369	368
1715	5.831	3.351	509	501
1712	5.841	3.326	489	486
1691	5.914	3.260	690	682
1681	5.949	3.228	765	767
1677	5.963	3.217	795	797
1650	6.061	3.134	1102	1096
1627	6.146	3.063	1214	1221
1621	6.169	3.043	1319	1321
1602	6.242	2.984	1534	1557

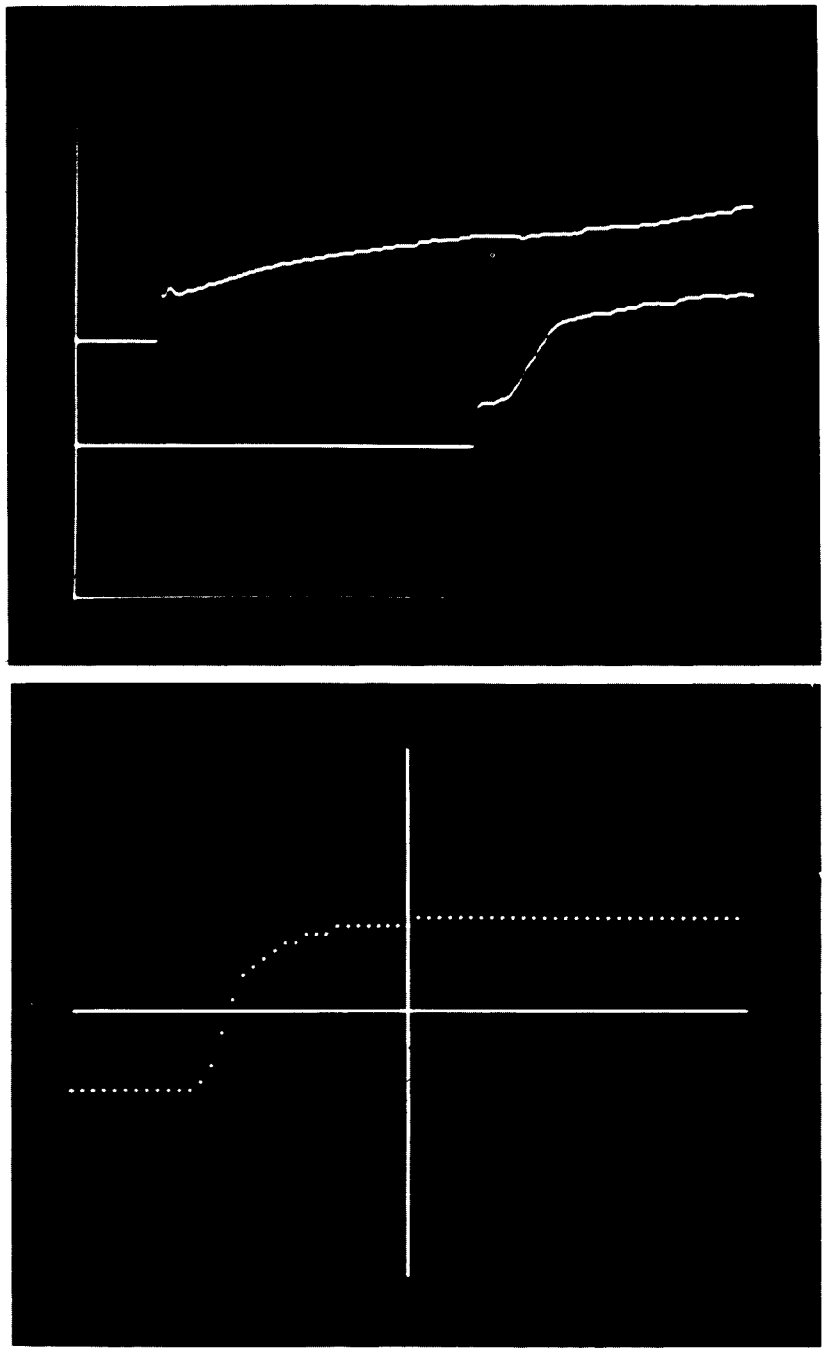

Figure 1. - Shock velocity measurement. Output from thin-film probe amplifier fed to digital oscilloscope. Time per point, 200 n sec. Lower trace shows expansion of scale, which is helpful in determining exact time shock wave passed probe position.

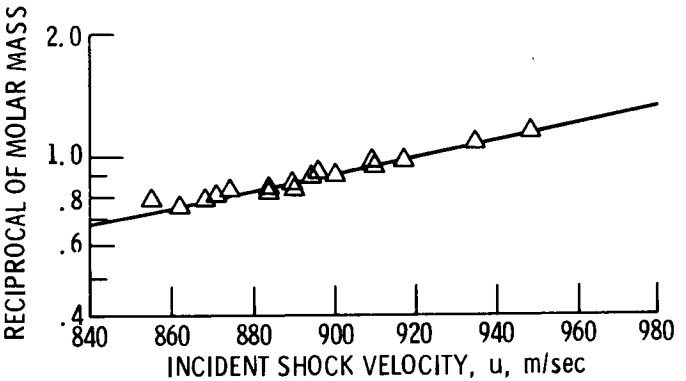

Figure 2. - Shock velocity as function of molar mass of driver gas for constant pressure ratio across diaphragm.

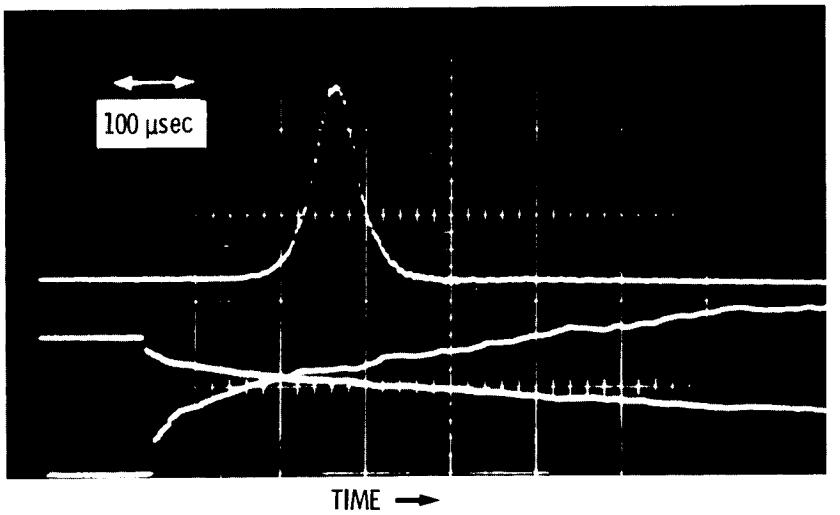

Figure 3. - Flame-band emission for mixture of hydrogen/oxygen/carbon monoxide/argon.

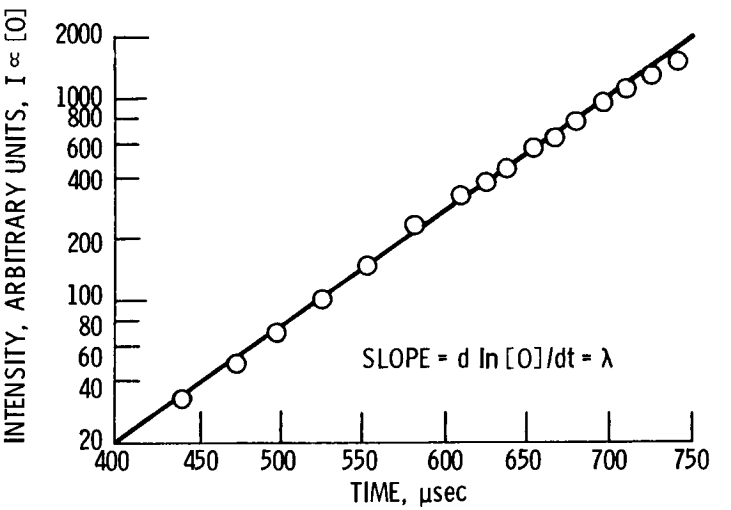

Figure 4. - Flame-band emission intensity as function of time.

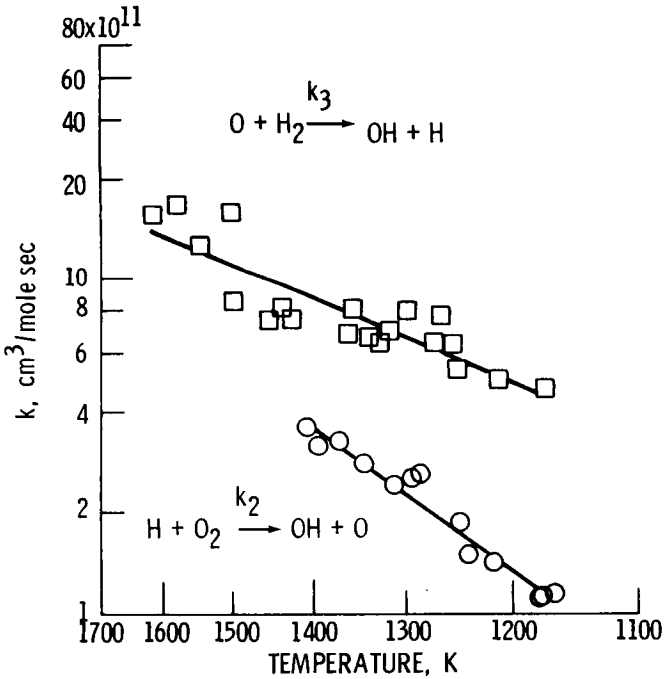

Figure 5. - Rate constants for reactions II and III. Solid lines indicate least-squares fit to experimental data.

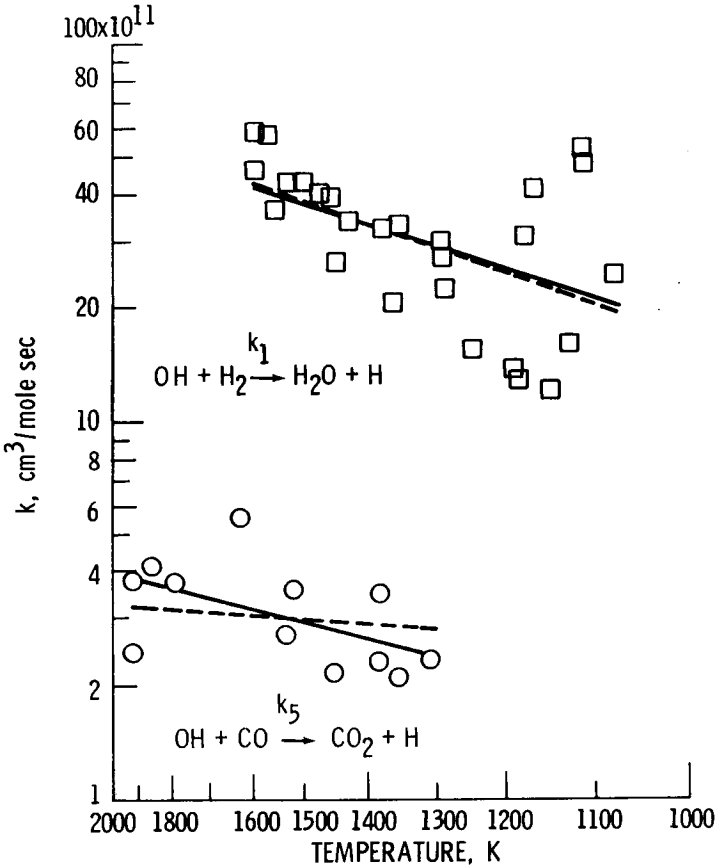

Figure 6. - Rate constants for reactions I and V. Solid lines indicate least squares fit to experimental data. Dashed lines indicate least-squares fit to experimental data plus 300 K datum of Greiner (ref. 13).

Figure 7. - Delay times measured at two locations in shock tube. Probes 1 and 2 are 7 and 83 mm from reflecting surface, respectively. P2 is incident shock pressure and P5 is reflected shock pressure. Measured delay times were 712 and 574 μsec.

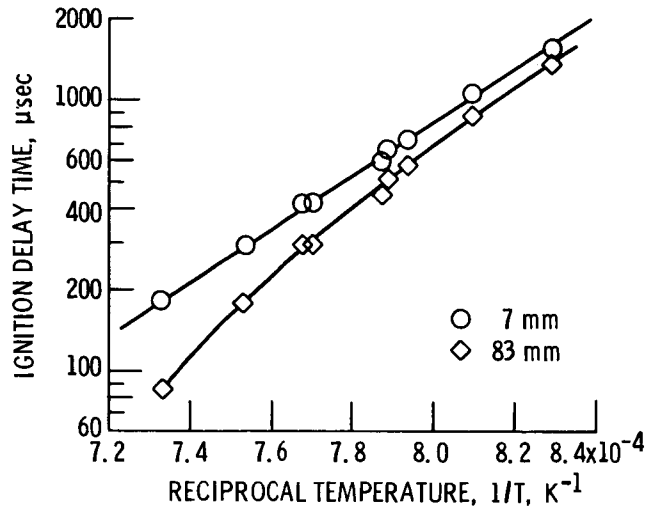

Figure 8. - Ignition delay times for a 1.27-percent C_2H_6, 5.05-percent O_2, 93.68-percent Ar (φ = 0.88) mixture as recorded at two different locations along shock tube.

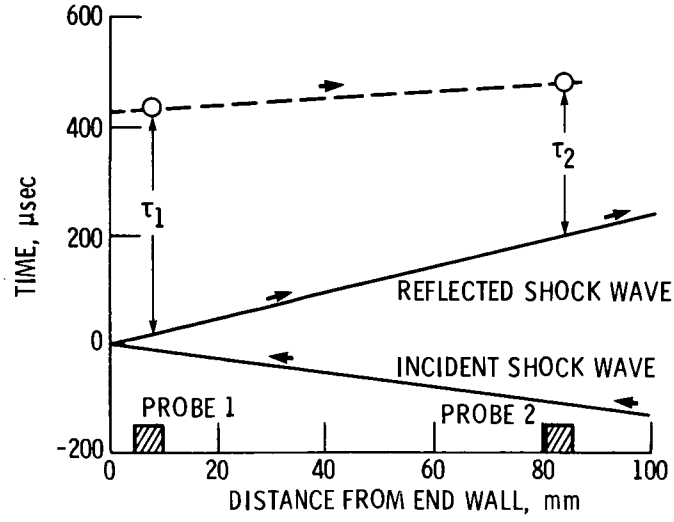

Figure 9. - Time-distance diagram of incident and reflected shock trajectory and delay times τ measured at two locations. Propagation of ignition wave shown by dashed line.

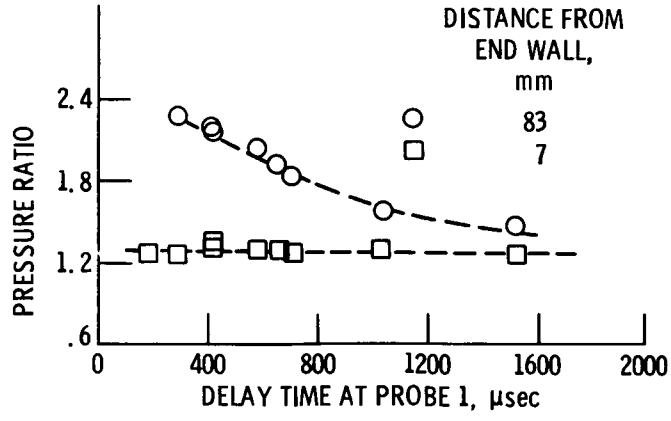

Figure 10. - Ratio of ignition pressure to reflected shock pressure, demonstrating enhanced ignition at second probe position, particularly for shorter delay times.

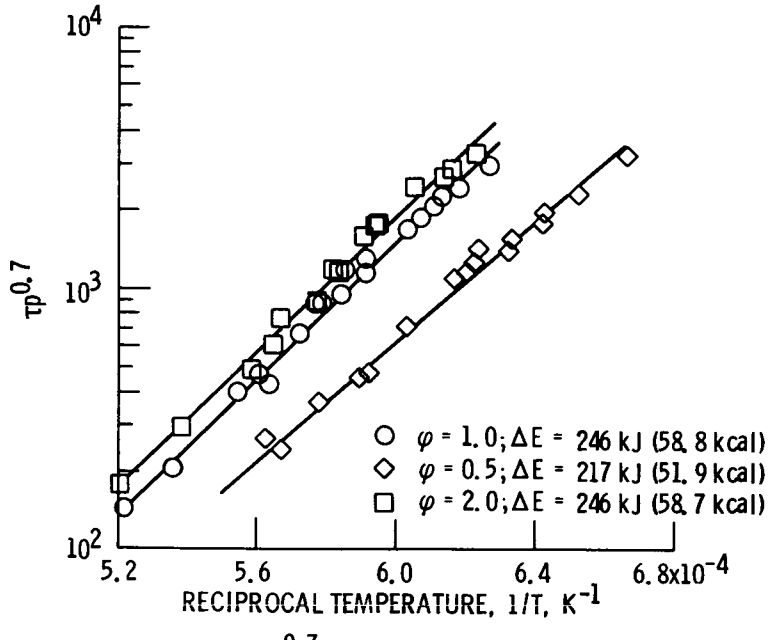

Figure 11. - $\tau p^{0.7}$ as function of 1/T for all three CH_4 mixtures, φ = 0.5, φ = 1.0, and φ = 2.0.